Melo, A. B. L., Panzera, T. H., Freire, R. T. S., & Scarpa, F. (2018). The effect of Portland cement inclusions in hybrid glass fibre reinforced composites based on a full factorial design. *Composite Structures*. https://doi.org/10.1016/j.compstruct.2018.01.069

ARTICLE IN PRESS

Composite Structures xxx (xxxx) xxx–xxx

Contents lists available at ScienceDirect

Composite Structures

journal homepage: www.elsevier.com/locate/compstruct

The effect of Portland cement inclusions in hybrid glass fibre reinforced composites based on a full factorial design

Arthur Bernardes Lara Melo[a], Túlio Hallak Panzera[a], Rodrigo Teixeira Santos Freire[a,b,*], Fabrizio Scarpa[c]

[a] Centre for Innovation and Technology in Composite Materials, Department of Mechanical Engineering, Federal University of São João del Rei – UFSJ, São João del Rei, Minas Gerais, Brazil

[b] Department of Natural Sciences, Federal University of São João del Rei – UFSJ, São João del Rei, Minas Gerais, Brazil

[c] Bristol Composites Institute (ACCIS), University of Bristol, UK

ARTICLE INFO

Keywords:
Hybrid composites
Full factorial design
Cross-ply glass fibre fabric
Epoxy polymer
Portland cement

ABSTRACT

The apparent density, flexural modulus and strength of hybrid laminated composites were investigated through a full-factorial Design of Experiment (DoE) approach. Laminates were manufactured by hand lay-up using nine layers of glass fibre cross-ply fabric with an epoxy matrix phase reinforced with Portland cement microparticles. A first experiment investigated the effect of the inclusion site (particles in upper four layers, lower four layers, all layers or none), curing time (7 and 28 days) and compaction method (vacuum or uniaxial pressure). The fibre–matrix volume fraction and the particle mass fraction were fixed at 48.6/51.4% and 10% respectively. A second experiment investigated two distinct fibre–matrix volume fractions (48.6/51.4 and 29.6/70.4%) and five particle mass fractions (0, 2.5, 5.0, 7.5 and 10 wt%). Particle inclusions were restricted to the upper four layers, with 28 days of curing time and uniaxial compaction. The results were analysed via Analysis of Variance (ANOVA). A significant increase in flexural modulus and strength was observed at 28 days of curing time. Enhanced mechanical properties were obtained for laminates with particle inclusions only in the upper half of the structure, manufactured with 48.6/51.4% fibre-matrix volume fraction and uniaxial pressure. Higher flexural strength was achieved for composites manufactured with 51/49% fibre–matrix volume fraction and 2.5% of particle mass fraction. These fibrous-particulate hybrid composite laminates can be considered for future secondary structural parts in lightweight engineering applications.

1. Introduction

Composite materials have been considered as substitutes for metallic materials, owing to their conformability and high specific mechanical properties. Composites have been used in a variety of applications in aerospace, automotive and construction industries owing to their low density and custom-engineered mechanical, thermal and acoustic properties [1,2]. Epoxy polymer is one of the most used thermosetting materials owing to its easy processing and fabrication, simple tooling and excellent adhesive and optically transparent properties [3]. The highly cross-linked polymeric structure of epoxy yields high elastic modulus and strength under tensile and compressive loads, but the tensile modulus and strength may be further increased using fibres.

Amongst all the applications of fibre-reinforced composites, laminated composites are the most common and in which fibres provide *in-plane* reinforcement. No reinforcement, however, is provided by fibres in the *transverse* direction and the resistance to delamination resides on the fracture toughness of the matrix itself. An effective technique to improve interlaminar fracture toughness of laminates is to increase the epoxy matrix toughness by adding micro - or nanosized fillers, such as soft rubber particles or rigid alumina and silica particles [4,5].

Particle inclusions can act as barriers against crack propagation and also enhance compressive modulus and strength of the matrix [6]. Particle size and weight fraction for matrix reinforcement are therefore selected to provide higher specific properties for the composite material [2]. Garg and Mai [7] extensively reviewed the toughening mechanisms of micro fillers in epoxy polymers. The toughening effect of silica nanoparticles on bulk epoxy has been already investigated in previous studies [8,9].

Particles may also increase, under proper conditions, the flexural modulus and strength. Such effect has been, however, much less investigated. Cao and Cameron [10] have reported an increase in flexural

* Corresponding author at: Centre for Innovation and Technology in Composite Materials, Department of Mechanical Engineering, Federal University of São João del Rei – UFSJ, São João del Rei, Minas Gerais, Brazil.

E-mail address: rfreire@ufsj.edu.br (R.T.S. Freire).

https://doi.org/10.1016/j.compstruct.2018.01.069
Received 15 January 2018; Accepted 19 January 2018

Please cite this article as: Melo, A.B.L., Composite Structures (2018), https://doi.org/10.1016/j.compstruct.2018.01.069

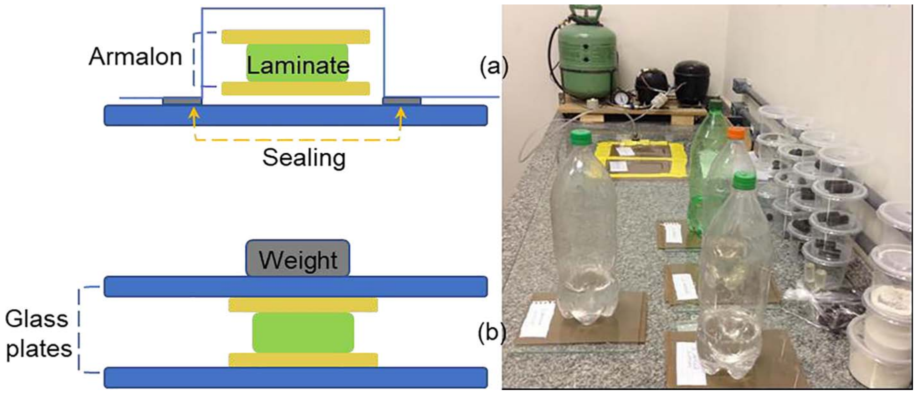

Fig. 1. Illustrations and experimental setup for the compaction methods: (a) vacuum and (b) uniaxial pressure.

Table 1
Experimental conditions studied in experiment A.

Experimental Conditions	Curing time (days)	Compaction method	Particle inclusion site
A1	7	Uniaxial	None
A2	7	Uniaxial	Upper half
A3	7	Uniaxial	Lower half
A4	7	Uniaxial	All layers
A5	7	Vacuum	None
A6	7	Vacuum	Upper half
A7	7	Vacuum	Lower half
A8	7	Vacuum	All layers
A9	28	Uniaxial	None
A10	28	Uniaxial	Upper half
A11	28	Uniaxial	Lower half
A12	28	Uniaxial	All layers
A13	28	Vacuum	None
A14	28	Vacuum	Upper half
A15	28	Vacuum	Lower half
A16	28	Vacuum	All layers

Table 2
Experimental conditions studied in experiment B.

Experimental Conditions	Fibre-matrix volume fraction (%)	Particle mass fraction (%)
B1	48.6/51.4	0.0
B2	48.6/51.4	2.5
B3	48.6/51.4	5.0
B4	48.6/51.4	7.5
B5	48.6/51.4	10.0
B6	29.6/70.4	0.0
B7	29.6/70.4	2.5
B8	29.6/70.4	5.0
B9	29.6/70.4	7.5
B10	29.6/70.4	10.0

modulus (approx. 10%) and strength (approx. 30%) of unidirectional glass fibre reinforced epoxy composites manufactured with silica microparticle-coated fibres relatively to uncoated fibres. Such improvement was associated to fibre-matrix interlocking effects.

Jeyakumar et al. [11] have also reported that nanoclay efficiently improved the flexural modulus and strength of glass fibre epoxy composites up to 5 wt% of nanoclay mass fraction, with a slight decrease in the flexural properties for higher particle mass fractions.

Detomi et al. [12] have investigated the effects of ceramic microparticle inclusions on the apparent density, flexural modulus and strength of glass fibre reinforced epoxy polymer composites under three-point flexural test. Silica or silicon carbide microparticles were added on the upper half or in the whole structure of five-layered laminates resulting in an increase of 112% in specific flexural strength when silica microparticles were incorporated at a 10 wt% level on the upper half of the laminate, relatively to non-particulate glass fibre laminates. The specific flexural modulus was however 26% lower.

Santos et al. [13] have reported that carbon fibre composites with silica nanoparticles presented higher flexural modulus (47%) and strength (15%) relatively to non-particulate composites, mainly when a 2 wt% particle mass fraction was used. These authors observed a good correlation between tensile and flexural modulus, which corroborates the observations that the increase in flexural modulus can be attributed to the stiffness increase of the reinforced matrix under tensile and compressive loadings [14,15]. Considering that particulate composites exhibit, in general, higher *compressive* stiffness and strength while fibrous materials exhibit higher *tensile* stiffness and strength, Torres et al. [16] have investigated the effects of silica and cement particle inclusions on hybrid glass fibre reinforced epoxy composites. Particle inclusions at the upper (under compression) beam side provided a significant increase in flexural modulus (19.60% for silica and 28.70% for cement particles). The highest flexural strength was achieved for composites fabricated with 5 wt% of cement particles. Cement particles were considered by these authors owing to experiment results reported in the literature concerning the hydration of cement particles in the presence of epoxy polymers.

A preliminary work, carried out in 1977 [17], on the use of Portland cement and other inorganic materials as fillers for different polymers, such as epoxy and polyester, considered the probabilities for chemical interaction between Portland cement and epoxides to be very low. The authors remarked that, up to that time, no evidence had been found for a real chemical interaction between epoxy polymer and Portland cement. However, Panzera et al. [18], based on infrared spectroscopy analysis, have reported compelling evidence of hydration of cement particles embedded in epoxy polymer, implying the formation of epoxy-portlandite hydrogen bonds. Soles and Yee [19] have in fact observed that water molecules penetrate the structure of the epoxy resin through a network of nanopores of 5.0 to 6.1 Å in diameter, which occupies 3 to 7% of the total volume of the cured polymeric structure. Water molecules can easily penetrate the structure, since the diameter of water molecules is much smaller (around 3.0 Å).

In this work, the potential enhancement of the flexural properties of hybrid glass fibre epoxy composites is investigated using cross-ply glass fibre fabrics in an effort to take advantage from the interlocking effect promoted by particles at the interlaminar region.

2. Material and methods

Hybrid composite laminates were manufactured by hand lay-up using nine layers of glass fibre cross-ply fabrics (Owens-Corning, 200 g/m^2) and Portland cement microparticles (diameter $< 44\,\mu m$, supplied by Lafarge-Holcim, Brazil). The matrix phase consisted of the epoxy polymer RenLam-M with the HY 951 catalyser (both supplied by Huntsman) at the proportion 5:1 (according to the manufacturer), mixed with cement microparticles according to the experimental

Table 3
Physical properties obtained from the thermogravimetric analysis.

Experimental Conditions	Apparent density (g/cm^3)		Volume fraction of voids (%)	Fibre-matrix	Volume fraction (%)
	Calculated	Measured		Calculated	Measured
A1	1.86	1.76	5.5	48.6/51.4	50.5/49.5
A5	1.87	1.77	5.2	48.6/51.4	50.9/49.1
A9	1.86	1.73	7.1	48.6/51.4	50.6/49.4
A13	1.91	1.79	6.2	48.6/51.4	53.9/46.1
B1	1.88	1.72	8.4	48.6/51.4	51.7/48.3
B6	1.71	1.65	3.3	29.6/71.4	39.1/60.9

Table 4
ANOVA for Experiment A.

	Experimental factors	Flexural modulus		Flexural strength		Apparent density	
		F-value	p-value	F-value	p-value	F-value	p-value
Main factors	Curing Time (CT)	65.09	0.000	209.32	0.000	2.47	0.135
	Compaction Method (CMP)	1.51	0.237	56.78	0.000	10.61	0.005
	Particle Inclusion Site (PIS)	6.88	0.003	20.27	0.000	6.16	0.005
Interactions	CT × CMP	0.68	0.423	0.02	0.903	0.42	0.525
	CT × PIS	3.60	0.037	4.18	0.023	0.30	0.827
	CMP × PIS	24.53	0.000	26.54	0.000	11.49	**0.000**
	CT × CMP × PIS	3.58	**0.038**	4.16	**0.023**	0.97	0.431
	R^2 (%)	91.96		96.43		81.45	
	p value (AD) ($p \geq 0.05$)	**0.427**		**0.651**		**0.516**	

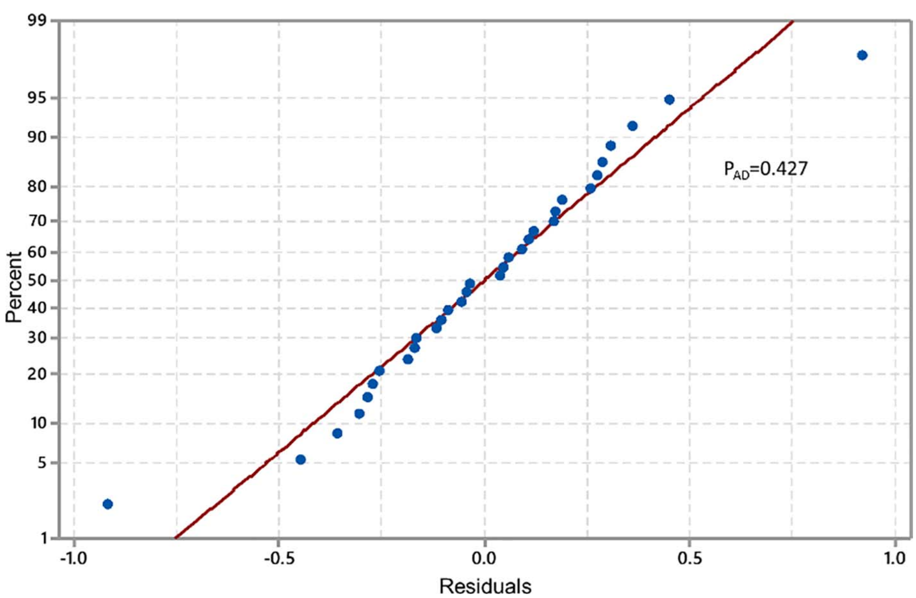

Fig. 2. Residual plot for the mean flexural modulus response.

conditions described below. Samples were cured under vacuum or uniaxial pressure at 0.9 bar (Fig. 1).

Two full factorial designs (A and B) were conducted [20,21] in order to evaluate apparent density, flexural modulus and flexural strength of the laminates. Three-point bending tests were conducted in accordance to ASTM-D790-10, using a Shimadzu Universal Testing Machine AGX-Plus with a 100 kN load cell, at a crosshead speed of 2 mm/min. Experiment A ($4^1 2^2$) evaluated the effects of particle inclusions on four different inclusion sites.

The particle mass fraction and fibre-matrix volume fraction were fixed at 10% and 48.6/51.4% respectively based on a previous work published elsewhere by this group [22]. The experimental conditions considered are listed in Table 1. Three samples were tested for each experimental condition with two replicates to a total of 96 samples.

Experiment B evaluated the effects of particle mass fraction (0, 2.5, 5.0, 7.5 or 10%) and fibre-matrix volume fraction (48.6/51.4 and 29.6/70.4%) via full factorial design $5^1 2^1$. Such fibre-volume fractions were selected based on preliminary tests performed to evaluate respectively the highest fraction to visually guarantee adequate wetting and finishing of the laminates, and the lower fraction that results in spontaneous resin leakage, in the absence of uniaxial or vacuum compaction. Based on results obtained from the Experiment A, only uniaxial pressure was used in experiment B, and particles were added only within the upper beam side (under compression), considering 28 days of curing time. The experimental conditions for experiment B are listed in Table 2.

Five samples were tested for each experimental condition with two replicates running a total of 90 samples for experiment B. The effects of

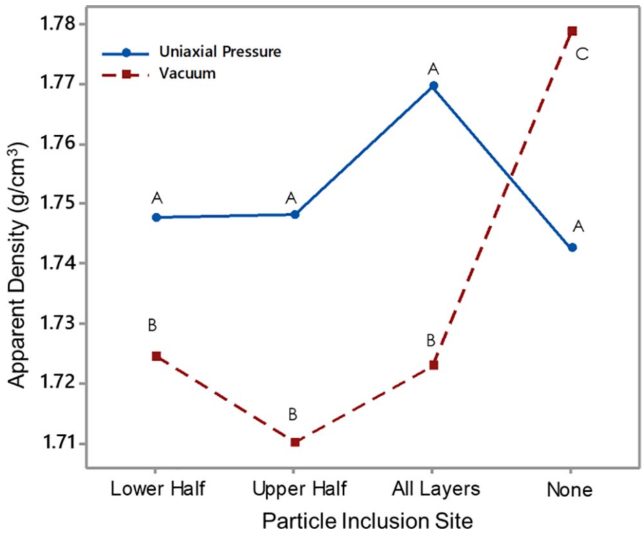

Fig. 3. Interaction effect plot for the mean apparent density response.

the different factors considered, and their interactions were studied through Analysis of Variance (ANOVA) [20,21].

3. Results

3.1. Thermogravimetric analysis

During fabrication, matrix leakage always occurs to some extent, and thus a thermogravimetric analysis (TGA) was performed to determine the experimental fibre-matrix volume fraction. Samples were extracted from test specimens and dried in an EDG 10P-S FC-2 electric oven. Starting at room temperature, composite samples were heated at 10 °C/min up to 600 °C for two hours followed with subsequent spontaneous cooling at room temperature. Such procedure incinerates the epoxy matrix so that only glass fibres remain. Only non-particulate samples were tested, since the volumetric fraction of ceramic particles and glass fibres could not be distinguished after thermal digestion. Such analysis was performed in two samples for each experimental condition and the calculated and experimental values for density and fibre-matrix volume fraction were compared (Table 3). The experimental fibre-matrix volume fraction was, as expected, higher than the respective calculated value, owing to matrix loss during the compaction method, either vacuum or uniaxial pressure. It is observed, however, in Experiment A, that vacuum (bold letters) implies higher resin leakage relatively to uniaxial compaction. The fraction of voids, however, was slightly higher when uniaxial compaction (underlined values) was used, except for B6, the experimental condition with lower fibre-matrix volume fraction, i.e., with higher matrix content. It is important to note that the fraction of voids can only be compared for the same curing time, since samples with distinct curing times belong to different batches. Calculations were based on ASTM-D792-08. The calculated fibre-matrix volume fractions considered for particulate composites were the same.

3.2. Three-point bending tests

3.2.1. Experiment A

The data obtained from the ANOVA analysis are summarized in Table 4. The particle mass fraction and fibre-matrix volume fraction were fixed at 10% and 48.6/51.4% respectively. The measured flexural modulus varied from 16.52 to 17.49 GPa and flexural strength results obtained varied from 355.24 MPa to 395.00 MPa.

The residual analysis for flexural modulus is presented in Fig. 2. Analogous results were obtained for flexural strength and apparent density and, for a matter of concision, will not be presented here. The Anderson-Darling normality test [20,21] presented p(AD)-values greater than 0.05, indicating that data follow a normal probability distribution, which is corroborated by the residual plot (Fig. 2), which resembles a straight line when the residual distribution is normal. Moreover, R^2 was greater than 81.45%, which implies that the data is well described by the underlying statistical model used for ANOVA. Both results therefore validate the ANOVA analysis.

The F-value is the ratio between the variance associated to the different levels of a given factor or interaction, and the variance within samples, which is due only to mere random chance. The F-value, used in conjunction with the p-value, therefore indicates how strongly a given factor influences the studied response [20,21] and it is seen that the curing time affects more strongly the flexural modulus (F = 65.09) and strength (F = 209.32), while the density is more strongly affected by the interaction of the compaction method and particle inclusion site (F = 11.49). For ANOVA, $p \le .05$ indicates that the factor significantly affects the considered response within a 95% confidence level. Such p-values are underlined in Table 4 and those in bold letters were

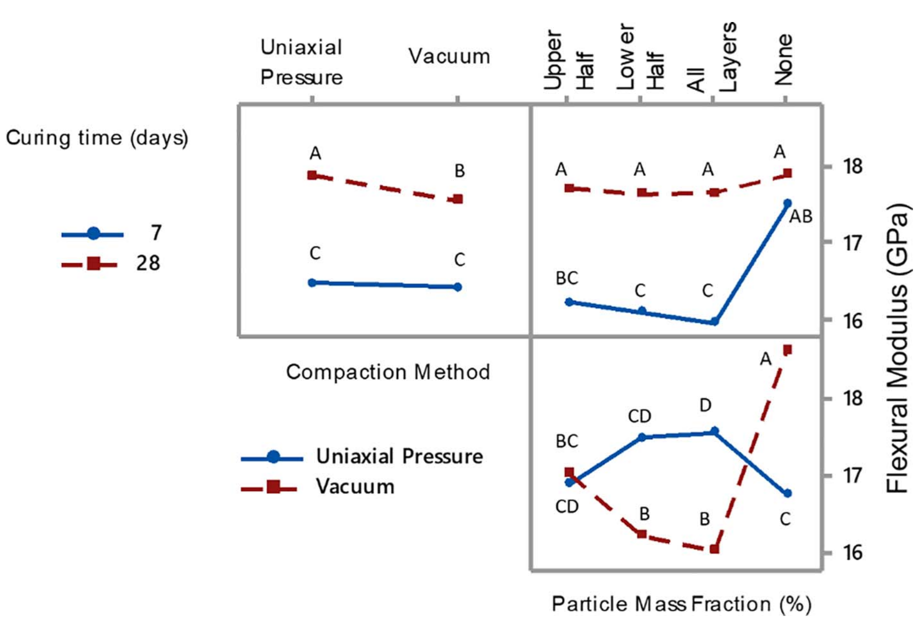

Fig. 4. Interaction effect plot for the mean flexural modulus response.

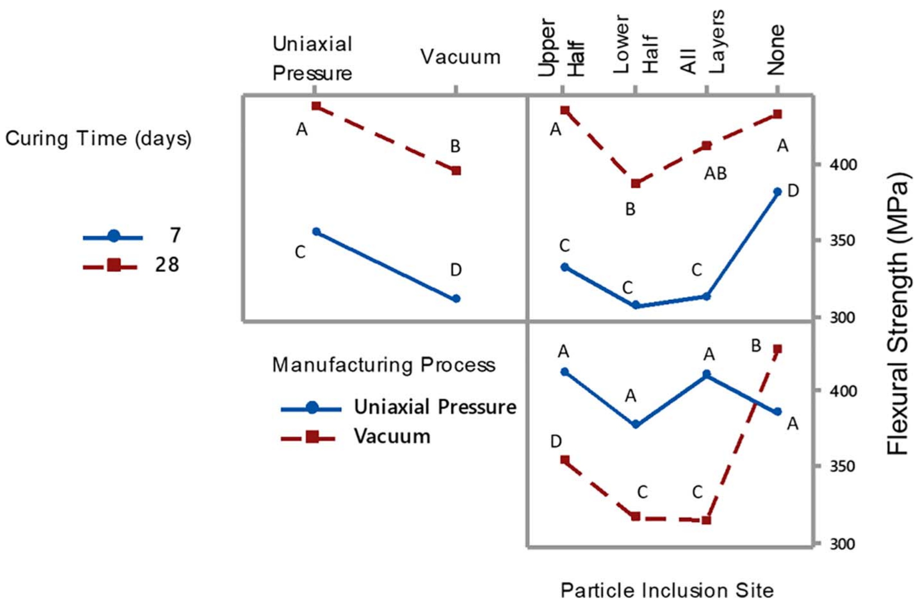

Fig. 5. Interaction effect plot for the mean flexural strength response.

Table 5
ANOVA for Experiment B.

	Experimental factors	Flexural modulus		Flexural strength		Apparent density	
		F-value	p-value	F-value	p-value	F-value	p-value
Main factors	Fibre-Matrix Volume Fraction (FMVF)	422.48	0.000	28.70	**0.000**	220.17	**0.000**
	Particle Mass Fraction (PMF)	3.12	0.066	5.15	**0.016**	1.78	0.210
Interaction	FMVF × PMF	5.27	**0.015**	1.38	0.307	5.05	0.017
	R^2 (%)	97.85		84.58		96.12	
	p value (AD) (p ≥ 0.05)	**0.938**		**0.837**		**0.750**	

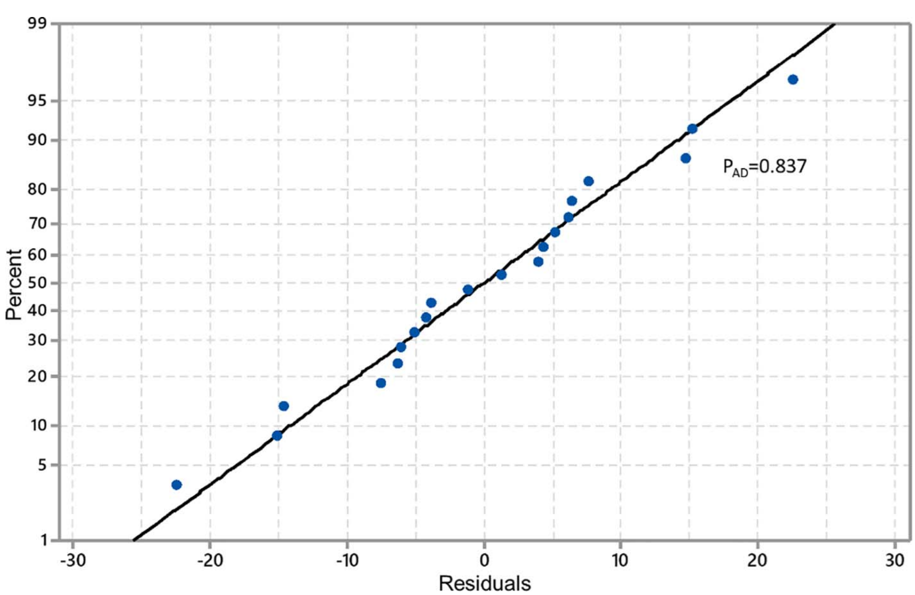

Fig. 6. Residual plot for the mean flexural modulus response.

interpreted via effect plots. It is important to note that the main effect of a given factor should be interpreted individually only when no interactions are identified.

Tukey's test is used to perform multiple comparisons in order to identify which mean values are different. The pair-wise comparison performed in Tukey's test [21] determines which pairs of mean values present a difference that is significantly higher than the standard deviation associated to mere stochastic error, considering a specific confidence interval. In this work a confidence interval of 95% was considered. In this case there is a probability of 5% that at least one pair of measures will be falsely found to be different. Tukey's test along with the letter coding describe above are used throughout all this work.

The interaction plot for the apparent density is depicted in Fig. 3. It is observed that the apparent density is significantly higher for non-

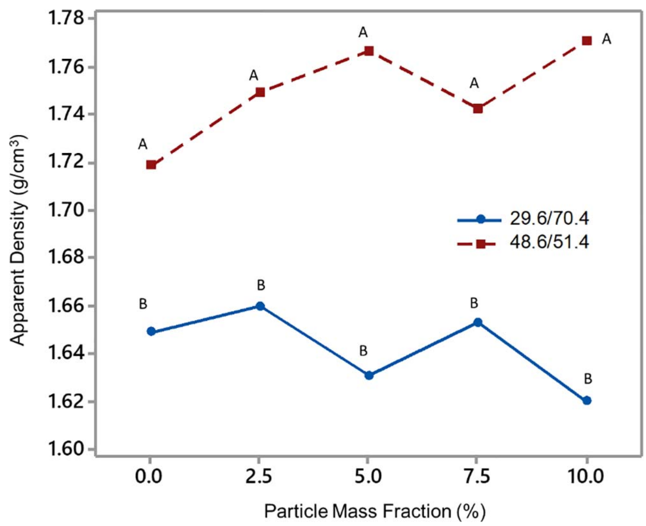

Fig. 7. Interaction effect plot for the mean apparent density response.

particulate laminates manufactured under vacuum, since voids are reduced under vacuum. Vacuum however expelled more resin, leading to significantly lower apparent densities. It is observed however, that upon uniaxial pressure, the apparent density is the same no matter what the inclusion site considered. Despite the increment when particles are included in all layers, the mean apparent densities for the particle inclusion sites considered are not statistically different, which is represented by the letters. Averages are statistically different when points do not share a common letter.

The interaction plot for flexural modulus is presented in Fig. 4. The curing time significantly enhanced the flexural modulus, which is, on average, 8% higher at 28 days. Vacuum manufacturing resulted in lower flexural modulus. Such behaviour may be explained by the fact that vacuum expelled a significant amount of resin (Table 3) when particles were included and hence lower stiffness, so that uniaxial pressure (no vacuum) is more adequate in this case. In the absence of particles, however, vacuum reduces voids increasing the apparent density and enhancing the flexural modulus. It worth noting that, for 7 days of curing time, particles decrease the flexural modulus; for 28 days of curing time, however, the flexural modulus increases significantly. This behaviour may suggest the building up of cement-matrix chemical interactions or cement hydration, as reported by Panzera et al. [18].

Similar behaviour is observed for the flexural strength (Fig. 5), which is on average 20% higher at 28 days. The flexural strength was approx. 5% higher for particle inclusions restricted only to the upper four layers or for non-particulate composites for 28 days of curing time. Although particles did not significantly influence the flexural strength when uniaxial pressure was used, particles significantly reduced the flexural strength when vacuum is used. This behaviour may be explained by the fact that more resin is expelled when vacuum is used, which leads to reduced interlaminar adhesion. As observed for the flexural modulus, uniaxial pressure (no vacuum) is therefore more adequate when particles are included. In the absence of particles, however, vacuum reduces voids, which increases the apparent density (Fig. 3) and enhances the flexural properties.

It is important to notice that non-particulate composites submitted to vacuum compaction present higher flexural modulus. Higher flexural strength (approx. 430 MPa) was equally obtained for non-particulate composites manufactured with vacuum or composites with particles on the top layers manufactured with uniaxial pressure. The particle mass fraction used in Experiment A, namely 10 wt%, is therefore clearly too high, and lower amounts of particles can significantly increase the flexural strength when included on the upper half of the laminate, which is investigated in Experiment B. Since more resin is expelled upon vacuum compaction in particulate composites, uniaxial compaction will be used.

3.2.2. *Experiment B*

At this stage, only uniaxial pressure was used, and particle inclusions were added only on the upper (under compression) half of the laminate, with 28 days of curing time. Results varied from 14.01 to 15.23 GPa (flexural modulus) and 408.70 to 409.76 MPa (flexural strength). The Anderson-Darling normality test presented p-values greater than 0.05, and the R^2 varied from 84.58% to 97.85%, which

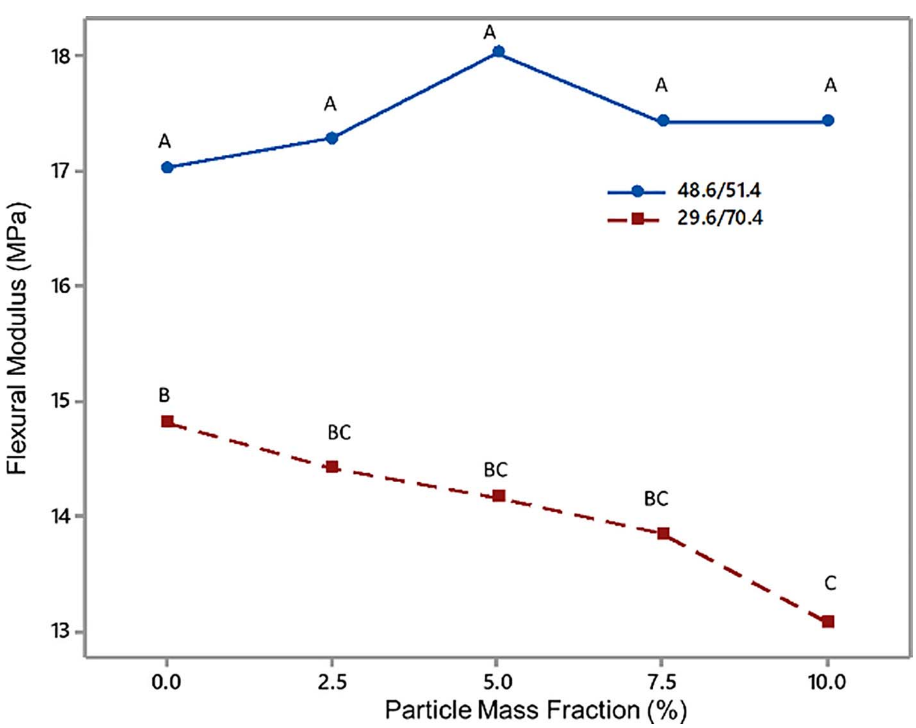

Fig. 8. Interaction effect plot for the mean flexural modulus response.

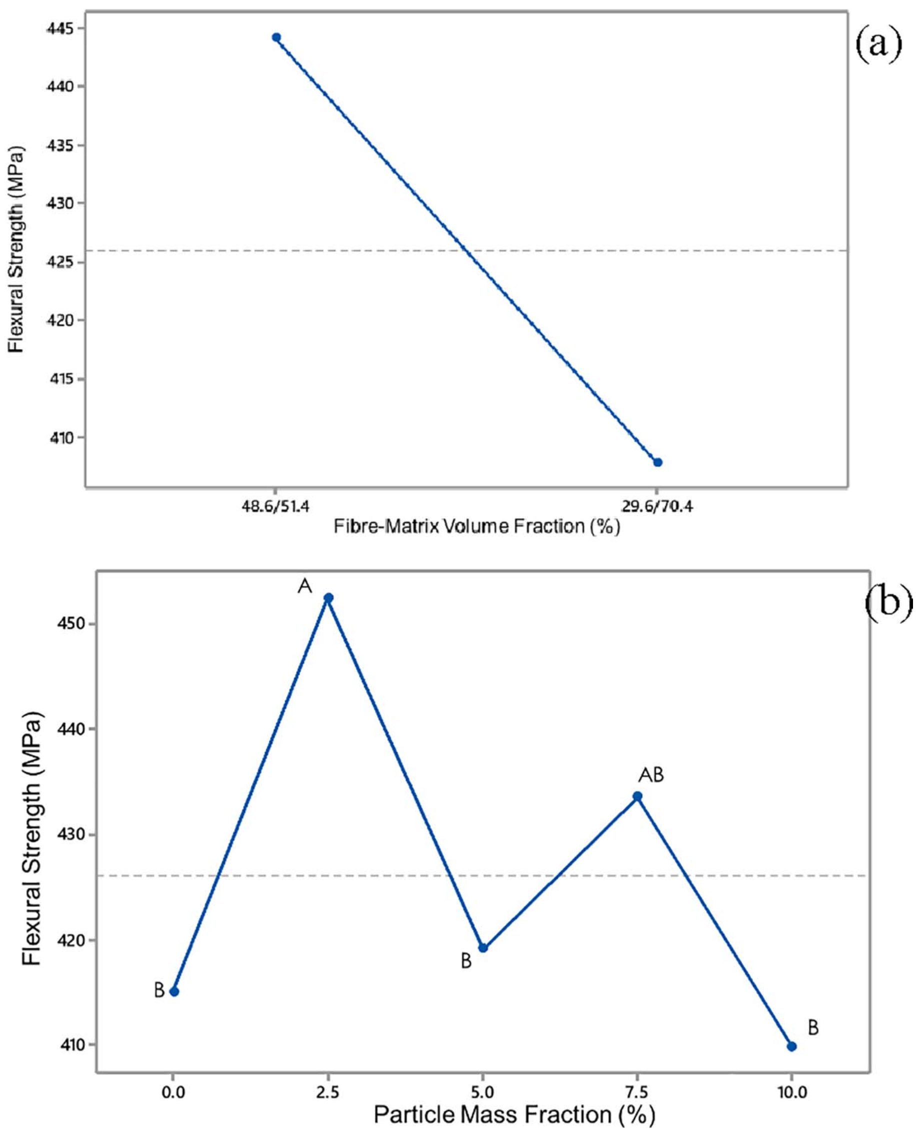

Fig. 9. Main effect plots of the factors (a) fibre matrix volume fraction and (b) particle mass fraction for the mean flexural strength response.

validates the ANOVA analysis, summarized in Table 5. The residual analysis for flexural strength is presented in Fig. 6. Analogous results were obtained for flexural modulus and apparent density and, for a matter of concision, will not be presented here.

The apparent density (Fig. 7) is not significantly affected by the particle mass fractions considered, but is higher, as expected, when the fibre-matrix volume fraction increases.

It is apparent (Fig. 8) that the flexural modulus is significantly higher for the higher fibre-matrix volume fraction considered (51/49.5%). It is however worth noting that cement particle inclusions reduced the flexural modulus when the lower fibre-matrix volume fraction was used, but such effect is not present when the higher fibre-matrix volume fraction was considered. The high fibre content on the lower half in fact tends to enhance the flexural modulus counterbalancing the effect of particles. Detomi et al. [12] have found a similar behaviour for silica and SiC particles on epoxy polymer fibre-reinforced laminates.

The flexural strength was also significantly higher for the higher fibre-matrix volume fraction considered (51/49.5%) (Fig. 9a) and for 2.5% of cement particle inclusions (Fig. 9b). It is however noteworthy that the specific flexural modulus obtained in this work (9–10 GPa.cm^3/g) was, on average, substantially higher than the obtained by Detomi et al. [12] (7.5 GPa.cm^3/g). In contrast, the specific flexural strength was significantly lower (250 MPa.cm^3/g) than the obtained by Detomi et al. (438 MPa.cm^3/g) [12].

4. Conclusions

The main conclusions are as following described:

i. Vacuum manufacturing expelled a significant amount of resin when particles were included, leading to lower interlaminar adhesion and hence, lower stiffness and strength, so that uniaxial pressure (no vacuum) is more adequate when particles are included. In the absence of particles, however, vacuum reduces voids and enhances flexural properties.
ii. The composites cured for 28 days exhibited higher flexural modulus and strength.
iii. Enhanced mechanical properties were obtained for laminates made with particles only in the upper half of the structure, manufactured with 51/49% fibre-matrix volume fraction and application of uniaxial pressure. The flexural strength was significantly higher for 2.5% of cement particle inclusions.
iv. The curing time sensitively affects the flexural modulus and strength when particles are included. This behaviour may suggest the building up of cement-matrix chemical interactions or cement hydration. This effect will be investigated in a posterior study.
v. Higher specific flexural modulus was obtained relatively to a

previous work by this group (Detomi et al. [12]) using silicon carbide (SiC) or silica microparticles, however, specific flexural strength was lower.

Acknowledgments

The authors would like to thank the Brazilian Research Agencies, CAPES, CNPq and FAPEMIG for the financial support provided.

References

[1] Sathishkumar TP, Satheeshkumar S, Naveen J. Glass-fibre-reinforced polymer composites - a review. J Reinf Plast Compos 2014;33:1258–75.
[2] Suresha B, Chandramohan G, Renukappa NM. Influence of silicon carbide filler on mechanical and dielectric properties of glass fabric reinforced epoxy composites. J Appl Polym Sci 2009;111:685–91.
[3] Dong Y, Chaudhary D, Ploumis C, Lau K-T. Correlation of mechanical performance and morphological structures of epoxy micro/nanoparticulate composites. Compos: Part A 2011;42:1483–92.
[4] Zeng Y, Liu H-Y, Mai Y-W, Du X-S. Improving interlaminar fracture toughness of carbon fibre/epoxy laminates by incorporation of nano-particles. Compos: Part B 2012;43:90–4.
[5] Kinloch AJ, Mohammed RD, Taylor AC. The interlaminar toughness of carbon-fibre reinforced plastic composites using 'hybrid-toughened' matrices. J Mater Sci 2006;41:5043–6.
[6] Fu S-Y, Feng X-Q, Lauke B, Mai Y-W. Effects of particle size, particle/matrix interface adhesion and particle loading on mechanical properties of particulate–polymer composites. Compos B 2008;39:933–61.
[7] Garg AC, Mai Y-W. Failure mechanisms in toughened epoxy resins - a review. Compos Sci Technol 1988;31:179–223.
[8] Johnsen BB, Kinloch AJ, Mohammed RD, Taylor AC, Sprenger S. Toughening mechanisms of nanoparticle-modified epoxy polymers. Polymer 2007;48:530–41.
[9] Tsai J-L, Hsiao H, Cheng Y-L. Investigating mechanical behaviors of silica nanoparticle reinforced composites. J Compos Mater 2010;44:505–24.
[10] Cao Y, Cameron J. Flexural and shear properties of silica particle modified glass fiber reinforced epoxy. J Reinf Plast Compos 2006;25:347–59.
[11] Jeyakumar R, Sampath PS, Ramamoorthi R, Ramakrishnan T. Structural, morphological and mechanical behaviour of glass fibre reinforced epoxy nanoclay composites. Int J Adv Manuf Technol 2017;93:527–35.
[12] Detomi AC, Santos RM, Ribeiro Filho SLM, Martuscelli CC, Panzera TH, Scarpa F. Statistical effects of using ceramic particles in glass fibre reinforced composites. Mater Des 2014;55:463–70.
[13] Santos JC, Vieira LMG, Panzera TH, Christoforo AL, Schiavon MA, Scarpa F. Hybrid silica micro and PDDA/nanoparticles-reinforced carbon fibre composites. J Compos Mater 2017;51(6):783–95.
[14] Zheng Y, Ning R, Ying Z. Study of SiO2 nanoparticles on the improved performance of epoxy and fiber composites. J Reinf Plast Compos 2005;24:223–33.
[15] Srinivasa V, Shivakumar V, Nayaka V, Jagadeeshaiaih S, Seethram M, Shenoy R, et al. Fracture morphology of carbon fiber reinforced plastic composite laminates. Mater Res 2010;13(3):417–24.
[16] Torres RB, Santos JC, Panzera TH, Christoforo AL, Borges PHR, Scarpa F. Hybrid glass fibre reinforced composites containing silica and cement microparticles based on a design of experiment. Polym Test 2017;57:87–93.
[17] Lerchental ChH, Brenman M. Inorganic particle-reinforced thermosetting resins. Composites 1977:93–9.
[18] Panzera TH, Sabariz ALR, Borges PHR, Vasconcelos DCL, Wasconcelos WL. Mechanical properties of composite materials based on Portland cement and epoxy resin. Cerâmica 2010;56:77–82.
[19] Soles C, Yee A. A discussion of the molecular mechanisms of moisture transport in epoxy resins. J Polym Sci, Part B: Polym Phys 2000;38:792–802.
[20] Montgomery DC, Runger GC. Applied statistics and probability for engineers. 6th ed. New York, NY, USA: John Wiley & Sons; 2014.
[21] Walpole RE, Myers RH, Myers SL, Ye K. Probability & statistics for engineers & scientists. 9th ed. Boston, MA, USA: Prentice Hall; 2012.
[22] Melo ABL, Paiva LFL, Santos JC, Silva LJ, Panzera TH, Freire RTS. A Statistical analysis of epoxy polymer reinforced with micro ceramic particles. J Res Updates Polym Sci 2016;5:108–13.